



D-BLAST MIMO PERFORMANCE ANALYSIS OVER SDR-USRP

ANÁLISIS DEL RENDIMIENTO DE D-BLAST MIMO SOBRE SDR-USRP

Freddy Cárdenas¹ , Jairo Otáñez¹ , Juan Inga^{2,*} ,
Esteban Inga³ , Andrés Ortega⁴

Received: 13-05-2021, Received after review: 29-11-2021, Accepted: 08-12-2021, Published: 01-01-2022

Abstract

This paper describes the implementation of the technique based on D-BLAST spatial multiplexing on Software Defined Radio (SDR) equipment. Specifically, the aim is to use Universal Software Peripheral Radio (USRP) Ettus Research x310 devices, to tackle the problem of spatial diversity of the MIMO Alamouti scheme which it is not able to increase the number of antennas of the transmitter with respect to the receiver. The simulation scenario was an indoor environment using LabVIEW Communications Software graphical programming tools, achieving a more robust coding design based on the nonlinearity of matrix equations, thus mitigating through the redundancy of information the effects of the interference due to the increase of the antennas of the transmitter. The experimental results evaluated were bit error rate (BER) and symbol error rate (SER) to determine the effectiveness of spatial diversity. The gain achieved was around 10dB and 7dB in MIMO 2×2 and MIMO 3×2, respectively, using the symmetric D-BLAST technique.

Keywords: Alamouti, D-BLAST, MIMO, SDR, USRP

Resumen

Este artículo describe la implementación de la técnica basada en multiplexación espacial D-BLAST sobre equipos de radio definido por *software* (SDR) específicamente usando USRP Ettus Research x310; con el objetivo de afrontar el problema de la diversidad espacial que posee el esquema de MIMO Alamouti, al no poder incrementar el número de antenas del transmisor respecto al del receptor. El escenario de simulación fue en un ambiente *indoor* usando las herramientas de programación gráfica con el *software Labview Communications*, logrando un diseño más robusto de codificación basado en la no linealidad de ecuaciones matriciales, mitigando, de este modo, a través de la redundancia de información los efectos de la interferencia que genera el incremento propio de las antenas en el transmisor. Los resultados experimentales evaluados fueron la tasa de error de bit (BER) y la tasa de error de símbolo (SER) para determinar la efectividad de la diversidad espacial. La ganancia lograda fue alrededor de 10 dB y 7 dB en MIMO 2×2 y MIMO 3×2 respectivamente, usando la técnica D-BLAST simétrica.

Palabras clave: Alamouti, D-BLAST, MIMO, SDR, USRP

¹Carrera de Ingeniería Electrónica / GITEL, Universidad Politécnica Salesiana, Cuenca, Ecuador.

^{2,*}Carrera de Telecomunicaciones / GITEL, Universidad Politécnica Salesiana, Cuenca, Ecuador.
Corresponding author ✉: jinga@ups.edu.ec

³GIREI, Universidad Politécnica Salesiana, Quito, Ecuador.

⁴Centro de Estudios y Desarrollo Sostenible (CEDS), Universidad Tecnológica ECOTEC, Guayaquil, Ecuador.

Suggested citation: Cárdenas, F.; Otáñez, J.; Inga, J.; Inga, E. and Ortega, A. "D-BLAST MIMO Performance Analysis over SDR-USRP," *Ingenius, Revista de Ciencia y Tecnología*, N.º 27, pp. 105-116, 2022, DOI: <https://doi.org/10.17163/ings.n27.2022.10>.

1. Introduction

The development of MIMO systems has gained increasing importance in recent years for standardization and implementation of modern communication systems. The challenges for obtaining high quality of service and high data rate are being exploited using MIMO techniques through multipath propagation, with the objective of increasing spectral efficiency in wireless channels. In this context, MIMO systems may also increase the capacity of the link exploiting channel diversity [1–5].

The spectrum is a scarce resource, and this is evident with spectral migration from LTE to 5G [2]. The mobile communication spectrum is already saturated in existing networks; consequently, the main benefits provided by MIMO techniques besides spatial diversity, are spatial multiplexing and current beamforming techniques deployed in intelligent antennas for spectral optimization.

A space-time coder such as Alamouti [6] scheme maximizes spatial diversity for an equal number of antennas at the transmitter and at the receiver. In spatial multiplexing, signals are transmitted and received simultaneously in the same frequency spectrum, at high data rates.

In this context, spatial diversity may be influenced in terms of Bit Error Rate (BER) by the number of antennas to the receiver. The experimental study reported in [6], demonstrates that the BER with fading channel is close to the ideal situation when the number of antennas in the receiver is increased. It should be also considered that the Alamouti space-time coder takes advantage of the spatial diversity presented by the multipath interference so that the receiver separates the received information symbols, which are mixed by the channel such that the energy of a symbol may be received by each of the receiver antennas. In the case of Alamouti, this may be achieved while the number of receiving antennas is equal to or larger than the number of transmitting antennas; however, this does not always occur.

1.1. D-BLAST Spatial Multiplexing

Spatial multiplexing (SM) by Space-Time layers known as BLAST (Bell Laboratories Layered Space-Time) are valid alternatives for MIMO data transmission. In addition, it should be indicated that spatial multiplexing known as D-BLAST enables the receiver to work in a MIMO scenario, where the number of transmitting antennas may be larger than the number of receiving antennas even though this would demand greater complexity in the design of the transmitter and the receiver [4], [7, 8]. According to this, the information symbols are demultiplexed in various layers each of which is transmitted independently. A rotation or di-

agonalization process of the information symbols is applied to achieve this, where each symbol corresponds to an independent data flow [9].

Consequently, it is necessary to consider that within BLAST architectures, D-BLAST proposes an architecture where the symbols to be transmitted are multiplexed by each of the antennas of the transmitter, i.e., at least in a time instant, an information symbol is transmitted by each of the transmitting antennas, which increases spatial diversity, an important factor to take advantage of MIMO. However, in contrast with other working formats such as Alamouti, D-BLAST enables considering the scenario where the number of antennas of the transmitter is greater than the number of antennas of the receiver, as previously mentioned [7, 8], [10, 11]. The MIMO D-BLAST system is chosen for this work due to its capacity to operate without knowledge of the state of the channel and its capacity to take advantage of spatial diversity [7], [12].

1.2. Implementation of MIMO techniques on SDRs

The Software Defined Radio (SDR) systems are radiocommunication systems that enable to implement modulations and physical layer transmission schemes through software [13]. In addition, the technological development of communication systems is marked by the design and use of FPGA prototyping systems [14] through Software Defined Radio (SDR) systems, where this hardware is controlled by means of different developing platforms. This gives flexibility to the evaluation of digital communication systems. In this development environment, many software platforms are enabling to access to the processing core of the FPGA with more flexibility, to handle digital signal processing (DSP) in the wireless communication system. Thus, the present work uses SDR equipment, concretely Universal Software Radio Peripheral (USRP) equipment [15, 16]. USRP programming has been carried out using graphical language, and they are increasingly taking control for parallel processing of signals in radio transmissions; LabVIEW Communications by National Instruments [16–18] was used for the development of this work.

For the case of MIMO systems, the scientific community has had much experimental development, being even able to test a MIMO with an array of 64 antennas [19]. This demands more hardware acquisition, and thus a higher implementation cost. For this reason, the development systems seek for platforms with more accessible costs for evaluating new technologies. For example, a 2×2 MIMO STBC-Alamouti scheme is evaluated in [20] through the use of USRP-2920 equipment employing the Simulink/MATLAB platform; it is verified the proportionality between the increment of the spatial capacity and the number of antennas of the

receiver, thus converging to a reduction in the BER through spatial diversity. However, Alamouti does not consider the case in which the number of antennas of the transmitter is larger than the number of antennas of the receiver.

The case presented in [12] is another example of modeling and application of MIMO systems, showing a MIMO D-BLAST implementation for air traffic communication systems. In such scenario, possible wireless interferences are greater than in an outdoor, indoor scenario, adding the interference (jamming) effect, situation which is common in the proposed scenario. In this way, [12] shows a strategy to unblock or disinhibit antennas due to the wireless interference, taking advantage of a MIMO system and using a low-speed feedback system for identifying the channel state; this aspect is indeed enabled by D-BLAST when facing the use of space-time coders. However, it should be considered that it is not always possible to take advantage of channel feedback since it requires an additional channel, and the system implemented is not either in contrast with the space-time encoding technique.

On the other hand, the use of the NI-USRP 2920 device [16] for MIMO systems has demonstrated that it is able to increase the capacity of the link; however, the system has two drawbacks due to the hardware architecture itself, namely (i) the data transmission rate, since the devices use the TCP/IP communication protocol, and (ii) when the number of antennas increases, it is necessary to use more SDR devices either for transmitting or receiving, thus arising a synchronization problem between devices. Case (i) may be improved using devices in which MXI ports are available for direct connection with the computer motherboard through the PCI-Express module. In this sense, although the speed improvement may be significant regarding transmission bandwidth, it is still limited. Case (ii) may be solved through software, to generate time synchronization signals from the first device to the second establishing a connection in a master-slave architecture using the corresponding inputs and outputs to pass the clock signals from one device to the other.

The synchronization problem is not only related to software, it is a software-hardware compromise which may be very complex. For example, in [16] the devices were synchronized using a LAN network between radio systems interconnected by means of a LAN switch. However, as the number of devices increases, the transmission rate decreases due to the capacity provided by the TCP/IP and the complexity of configuring the synchronization of devices increases. It should be remarked that this synchronization refers to all devices that constitute the transmitter or the receiver, and not to the synchronization of the communication link, which in this work is solved using training symbols in the transmission frame. This is expanded in subsequent sections. As mentioned above, a simpler option but also of higher cost is to use a version that integrates

a MIMO array, as it is the case with the NI-USRP 2940R model equivalent to the devices USRP Series X300. This SDR model already implements a 2×2 array of antennas, simplifying the system implementation process and enabling to concentrate in processing the baseband radio signals and the digital communication section of the communication system. In addition, this model integrates the MXI port to increase the communication bandwidth between the SDR and the computer.

If the number of devices is larger than two, it is simpler to solve the synchronization problem using an external clock signal controller, such as the GPS NI-CDA2990 device. Since this work evaluates communication systems where the number of transmitting antennas is greater than 2, external synchronization is used because more than two devices are being used in the transmitter; therefore, the use of the NI-CDA2990 device is important in the MIMO operation and, hence, evaluation. Figure 1 shows an image corresponding to the implementation of this work using the aforementioned devices, where it can be seen how the SDR devices are arranged. It should be also mentioned that the use of this external clock may limit the distance of the link if it is used both in the transmitter and in the receiver.

1.3. Object of study and hypothesis

The object of study is mainly focused on the design and implementation of the nonlinear matrix equations in the D-BLAST coder, using 3 methods to improve symbol detection in the receiver: (i) Average the symbols transmitted at the different positions of the columns where each symbol is repeated, since it is distributed diagonally with the interference of other symbols; (ii) Equal to method (i), but the interference is subtracted, and finally (iii) Knowing that the largest interference is at the medium column of the matrix, this column is neglected and the remaining columns are averaged, likewise the aforementioned methods. The objective is to compare through a practical implementation with SDR devices, the performance between MIMO schemes such as diagonal spatial multiplexing or D-BLAST and Alamouti space-time coder (STBC) implemented in a real indoor environment using USRP equipment, as opposed to what was implemented [21], where the BLAST spatial multiplexing is evaluated, but in vertical format.

The rest of the paper is structured as follows: section II carries out a review of works similar in the use of SDR devices. Section III analyzes the scheme and mathematical model of the D-BLAST space-time coder and describes the implementation process of the decoding algorithms used in the SDR devices. Section IV presents the results obtained, analyzing the figures of merit such as the bit error rate. The document end with the conclusions presented in section V.



Figure 1. Equipment implementation

2. Materials and methods

The equipment considered for implementing the MIMO system architecture are the USRP X310 devices of the Ettus Research company, due to the transmission rate flexibility of every radio device. This device model has a PCI-E port to transmit up to 1 Gbps; in addition, it has an external GPS disciplined oscillator (GPSDO) synchronization system, and using the NI-CDA2990 synchronization clock it is possible to expand up to 8 antennas in the transmitter and in the receiver. LabVIEW NI Communications was the software development platform, which facilitates the synchronization process for any communication system that requires more than two transmitting or receiving equipment. Thanks to synchronization, each of the devices may establish the same symbol, bit and/or sample time.

The CDA-2990 device enables to distribute a clock signal to connect up to 8 channels or SDR equipment. This device may externally generate a synchronization clock pulse by GPSDO or through a crystal that enables to generate input synchronization signals with pulse per second (PPS) precision. The configuration and connection used in this work is shown in Figure 2.

2.1. D-BLAST Spatial Multiplexing Architecture

It is an architecture that combines various equal or similar signals with low bandwidth to obtain a signal with larger bandwidth [22, 23]. In addition, similar to

how it occurs in space-time coding, data are transmitted simultaneously through each antenna and through each channel [4], [22]. However, D-BLAST spatial multiplexing uses flow of intertwined data symbols; it should be taken into account that symbols might have been obtained from a flow of bits to which any coding or forward error correction (FEC) technique was previously applied.

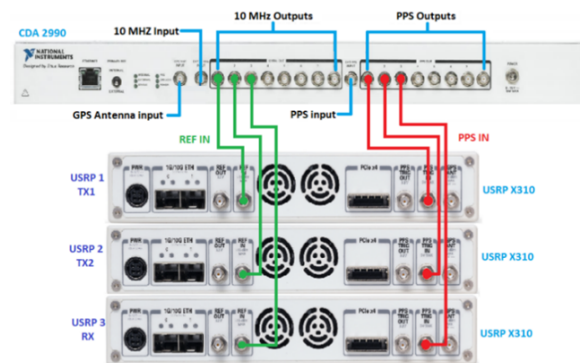


Figure 2. Connections of the CDA-2990, device used for the synchronization of NI-USRP radio devices

Based on this, it is first necessary to organize the information bits to be transmitted by means of a series/parallel converter according to the number of antennas of the transmitter. Then, time coding is applied to each flow obtained from the series/parallel conversion, and subsequently symbol mapping or linear modulation is used, as seen in Figure 3.

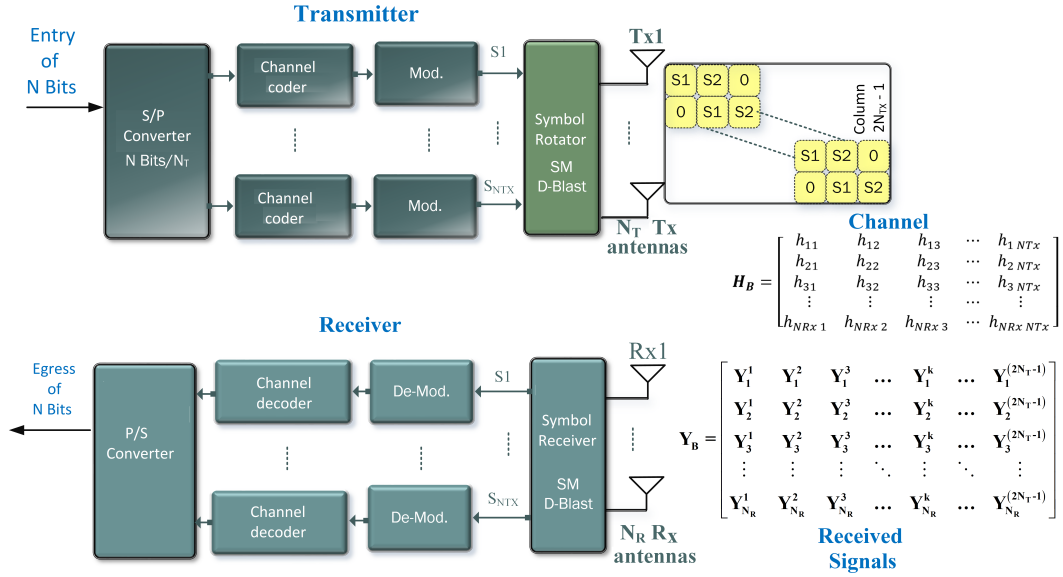


Figure 3. D-BLAST Spatial Multiplexing Architecture

In this way, independent frames are created for each antenna of the transmitter prior to the spatial multiplexing process, where these frames pass through a block that diagonally rotates the symbols of each flow [24] so that each symbol is transmitted at least one time through each of the antennas at the transmitter to ensure spatial diversity.

To illustrate this process, consider a transmitter with $N_T = 3$ antennas; in this way it is assumed that prior to space-time multiplexing, i.e., at the input of the block that rotates the symbols, there will be one symbol for each flow generally represented as the i -th symbol that enters this rotator. On the other hand, the output will be represented by equation 1, where the positions filled with «0» correspond to time instants where no information is transmitted, i.e., signals with zero energy. In this way, each symbol hops from one antenna to the other at each transmission time T_k .

$$S_D = \begin{pmatrix} s_1^1 & s_2^2 & s_3^3 & 0 & 0 \\ 0 & s_1^1 & s_2^3 & s_3^4 & 0 \\ 0 & 0 & s_1^3 & s_2^4 & s_3^5 \end{pmatrix} \quad (1)$$

The columns of equation (1) represent each of the transmission instants or times, while the rows correspond to transmitting antennas. Thus, s_3^3 corresponds to symbol 2 transmitted at time instant 3 or T_3 and, in general, s_i^j represents symbol i that entered the rotator and will be transmitted at time j . Then, for a D-BLAST diagonal spatial multiplexing, the dimension of the resulting symbol rotation matrix at the transmitter will be N_T rows \times $2N_T - 1$ columns, understanding that each group of symbols enter and are mapped independently according to the space-time matrix applying the symbol rotation described in general

by equation (2).

$$S_D = \begin{pmatrix} s_1^1 & s_1^2 & \dots & s_{N_T}^{N_T} & 0 & \dots & 0 \\ 0 & 0 & \dots & s_{N_T}^{N_T-1} & s_{N_T+1}^{N_T} & \dots & 0 \\ 0 & 0 & \dots & s_{N_T}^{N_T-2} & s_{N_T+1}^{N_T-1} & \dots & 0 \\ \vdots & \vdots & \ddots & \vdots & \vdots & \ddots & \vdots \\ 0 & 0 & \dots & s_1^{N_T} & s_1^{N_T+1} & \dots & s_{N_T}^{2N_T-1} \end{pmatrix} \quad (2)$$

The matrix \mathbf{H}_B with channel coefficients is shown in equation (3) and the matrix of signals received is \mathbf{Y}_D obtained according to equation (4), which is a function of the \mathbf{H}_B channel of the \mathbf{S}_D symbols transmitted and of the noise of the channel represented by \mathbf{n} . For \mathbf{H}_B , the element $h_{i,j}$ represents the impulse response of the channel between the transmitting antenna i and the receiving antenna j .

$$H_B = \begin{pmatrix} h_{11} & h_{12} & h_{13} & \dots & h_{1N_T} \\ h_{21} & h_{22} & h_{23} & \dots & h_{2N_T} \\ \vdots & \vdots & \vdots & \ddots & \vdots \\ h_{N_R \times 1} & h_{N_R \times 2} & h_{N_R \times 3} & \dots & h_{N_R \times N_T} \end{pmatrix} \quad (3)$$

$$\mathbf{Y}_D = \mathbf{H}_B \mathbf{S}_D + \mathbf{n} \quad (4)$$

For a continuous transmission, prior to applying the rotator a matrix is formed with the information symbols to be transmitted, where the number of rows is N_T and the number of columns is $(R \cdot N)/N_T$, where N represents the number of information bits and R is the FEC coding rate. In this way, according to the

mentioned example with $N_T = 3$, the second column that enters the rotator corresponds to symbols s_4 , s_5 and s_6 , which means that the rotator working matrix would use the following 5 transmission time instants under the matrix format given by equation (1) independent of the first three symbols.

Regarding reception, according to equation (4), for each symbol time it is received a linear combination of the symbols transmitted at time instant T_k through channel \mathbf{H}_B with elements $h_{i,j}$; this means that each antenna of the receiver contains information of all symbols at such time instant T_k .

On the other hand, Table 1 shows the arrangement of symbols to be transmitted considering the 2×2 MIMO case, presenting the rotation of D-BLAST symbols transmitted for each time instant and for each antenna for the first two transmission blocks; for the case of the D-BLAST 2×2 MIMO reception, Table 2 shows the position of the symbols received for the first two blocks, identifying the corresponding symbol times.

Table 1. Arrangement of Symbols for TX with D-BLAST 2×2 MIMO

	T_1	T_2	T_3	T_4	T_5	T_6
Antenna T_{X1}	s_1^1	s_2^2	$\mathbf{0}$	s_3^4	s_4^5	$\mathbf{0}$
Antenna T_{X2}	$\mathbf{0}$	s_1^2	s_2^2	$\mathbf{0}$	s_3^5	s_4^6
	First TX Block for 2×2 MIMO			Second TX Block for 2×2 MIMO		

Table 2. Arrangement of Symbols for RX with D-BLAST 2×2 MIMO

	T_1	T_2	T_3	T_4	T_5	T_6
Antenna R_{X1}	Y_1^1	Y_1^2	Y_1^3	Y_1^4	Y_1^5	Y_1^6
Antenna R_{X2}	Y_2^1	Y_2^2	Y_2^3	Y_2^4	Y_2^5	Y_2^6
	First RX Block for 2×2 MIMO			Second RX Block for 2×2 MIMO		

Each of the symbols or signals received described in Table 2 correspond to signals exiting the channel, which are detailed in equations (5) to (10), where equation (5) corresponds to the signals received at the first-time instant for both antennas 1 and 2 of the receiver of the proposed example.

$$Y_1^1 = h_{11}s_1^1 + h_{12} \cdot 0 + n_1 \quad Y_2^1 = h_{21}s_1^1 + h_{22} \cdot 0 + n_2 \quad (5)$$

$$Y_1^2 = h_{11}s_2^2 + h_{12}s_1^2 + n_3 \quad Y_2^2 = h_{21}s_2^2 + h_{22}s_1^2 + n_4 \quad (6)$$

$$Y_1^3 = h_{11} \cdot 0 + h_{12}s_2^3 + n_5 \quad Y_2^3 = h_{21} \cdot 0 + h_{22}s_2^3 + n_6 \quad (7)$$

$$Y_1^4 = h_{11}s_3^4 + h_{12} \cdot 0 + n_7 \quad Y_2^4 = h_{21}s_3^4 + h_{22} \cdot 0 + n_8 \quad (8)$$

$$Y_1^5 = h_{11}s_4^5 + h_{12}s_3^5 + n_9 \quad Y_2^5 = h_{21}s_4^5 + h_{22}s_3^5 + n_{10} \quad (9)$$

$$Y_1^6 = h_{11} \cdot 0 + h_{12}s_4^6 + n_{11} \quad Y_2^6 = h_{21} \cdot 0 + h_{22}s_4^6 + n_{12} \quad (10)$$

2.2. D-BLAST using Software Defined Radio (SDR) Systems

The block diagram of the communication system implemented on Universal Software Radio Peripherals (USRP) is shown in Figure 4. The UHD architecture used is the one available for «LabVIEW Communication Design Suite». The devices used were the USRP Ettus X310 with the following specifications:

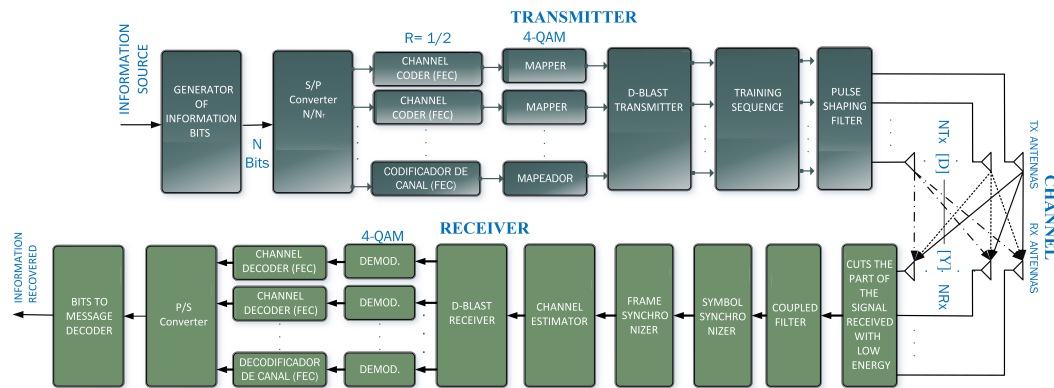


Figure 4. D-BLAST Implementation Architecture on SDR-USRP devices

- Bandwidth up to 40 MHz per channel (2 channels).
- The image loaded in the FPGA enables a 1 Gbps Ethernet connection to transmit 25Mega samples/s Full Duplex.
- Flexible clock architecture with configurable sampling frequency.

For MIMO implementation with SDR devices, the Alamouti 2×2, D-BLAST 2×2 and D-BLAST 3×2 configurations were used, where the information source is based on text, therefore, a source coder was implemented to obtain the appropriate flow of information bits. The first block of the transmitter in Figure 4 represents such source coder. In the case of application of the D-BLAST architecture, the flow of bits obtained from the information source is transformed from series to parallel according to the number N_T of transmitting antennas. For the case of this work, $N_T = 2$ and $N_T = 3$ and $N_R = 2$ for both cases.

After obtaining multiplexed flows of bits, a channel coder with a structure similar to the one used in Alamouti and also the same 4-QAM modulation scheme were applied to each sub-flow, in order to make no difference when comparing the results. In this architecture, the time coding and modulation process is independent for each data sub-flow. D-BLAST is applied to these sub-flows.

Training symbols are inserted at the output of the D-BLAST transmission block so that the receiver may synchronize the data frames received in each sub-flow. The training symbols are transmitted sequentially by each of the antennas in the array, but the sequence of each sub-flow is transmitted individually. Therefore, for the case of the 3 × 2 example, the sub-flow consists of three parts, one constituted by symbols in the $\pm \frac{1}{\sqrt{2}} \pm \frac{1}{\sqrt{2}}i$ range, and the other two correspond to symbols at zero ($0 + 0i$). Then, the set of symbols that constitute the preamble of each sub-flow contained 528 symbols, where each of the parts previously described contains 176 symbols. The arrangement of these training symbols is presented in Table 3. This structure will enable that the training sequence of each data sub-flow does not interfere with another, and the communication is more stable.

Table 3. Distribution of the training symbols in the sub-flows

sub-flow 0	$\pm \frac{1}{\sqrt{2}} \pm \frac{1}{\sqrt{2}}i$	0+0i	0+0i	S_D
sub-flow 1	0+0i	$\pm \frac{1}{\sqrt{2}} \pm \frac{1}{\sqrt{2}}i$	0+0i	
sub-flow 2	0+0i	0+0i	$\pm \frac{1}{\sqrt{2}} \pm \frac{1}{\sqrt{2}}i$	
Total length = 528 symbols				

In the blocks shown at the receiver, five additional blocks are applied unlike the simulation diagram. According to this, the first receiver block in Figure 4 seeks to eliminate low energy samples that correspond to filling symbols set equal to zero. For this purpose, a threshold level is established to enable discarding samples with very low energy or simply noise. In this way, the threshold is the average energy of all possible values that may be obtained in a digital modulation. In the case of this work, it is the average of the four possible symbols transmitted with 4-QAM.

The second block is a coupled filter to maximize the Signal-to-Noise (SNR) of the signals captured. The third and fourth blocks of the receiver are in charge of synchronizing the symbol time and synchronizing a frame due to the signals captured by each of the antennas of the receiver. To achieve this, it is exploited that the receiver knows the training symbols, which are known by the receiver, and are eliminated at the output of the receiver. The mathematical model for each signal received before eliminating the synchronization symbols is presented in Table 4 and Table 5 for constructing the 2×2 MIMO and 3×2 MIMO, respectively; in both cases, these expressions result applying equation (4). Prior to using this third block of the receiver, the appropriate symbol sub-sampling is applied to pass from samples to symbols and, therefore, when finalizing the synchronization, the symbols that are ready for channel estimation are obtained at the output of the fourth block of the receiver.

The channel estimator block has a number of inputs equal to the number of transmitting antennas. In addition, to estimate the channel coefficients, it was decided to use an estimator of low computational complexity based on least squares (LS) [25, 26]. As mentioned above, the channel estimation used in this work requires that the receiver knows the symbols used for synchronization and has the objective function described by the equation $\mathbf{h}_{LS} = \arg \min_h \|\mathbf{y} - \widehat{H}\mathbf{A}\|$ where the training symbols sequences transmitted are defined as $\mathbf{A} \in \mathbb{R}^{N_{TX} \times L}$, and the expression of the received matrix of training sequences is \mathbf{y} .

Table 4. Signals received for 2×2 MIMO considering the first layer of symbols for D-BLAST

	\mathbf{T}_1	\mathbf{T}_2	\mathbf{T}_3
\mathbf{R}_{x1}	$s_1 h_{11} + \mathbf{n}$	$s_1 h_{11} + s_1 h_{12} + \mathbf{n}$	$s_2 h_{12} + \mathbf{n}$
\mathbf{R}_{x2}	$s_1 h_{21} + \mathbf{n}$	$s_2 h_{21} + s_1 h_{22} + \mathbf{n}$	$s_2 h_{22} + \mathbf{n}$

Table 5. Signals received for 3×2 MIMO considering the first layer of symbols for D-BLAST

		T_1	T_2	T_3	T_4	T_5
Y_B	R_{X1}	$s_1 h_{11}$ + \mathbf{n}	$s_2 h_{11}$ + $s_1 h_{12}$ + \mathbf{n}	$s_3 h_{11}$ + $s_2 h_{12}$ + $s_1 h_{13}$ + \mathbf{n}	$s_3 h_{12}$ + $s_2 h_{13}$ + \mathbf{n}	+ $s_3 h_{13}$ + \mathbf{n}
	R_{X2}	$s_1 h_{21}$ + \mathbf{n}	$s_2 h_{21}$ + $s_1 h_{22}$ + \mathbf{n}	$s_3 h_{21}$ + $s_2 h_{22}$ + $s_1 h_{23}$ + \mathbf{n}	$s_3 h_{22}$ + $s_2 h_{23}$ + \mathbf{n}	+ $s_3 h_{23}$ + \mathbf{n}

In other words, the *LS* estimation algorithm seeks to find the \mathbf{h}_{LS} coefficients of the estimated channel \widehat{H} that minimize the quadratic error between the synchronization symbols received and the approximate version that uses the symbols known by the receiver. In addition, since the training symbols are known by the receiver, it is possible to pre-calculate matrix A^\dagger and store it in memory, and consequently the receiver does not calculate the pseudoinverse of \mathbf{A} every time the channel is re-estimated $\widehat{H} = A^\dagger \mathbf{y} = (\mathbf{A}^H \mathbf{A})^{-1} \mathbf{A}^H \mathbf{y}$.

At the output of the estimator, the training sequences are withdrawn and with the channel estimated and the symbols synchronized the received symbols are separated, because due to the channel multipath typical of a MIMO transmission, the information of each symbol transmitted during each transmission block (see Table 1) is now in all the received symbol flows.

2.2.1. D-BLAST Space-Time Decoder or Demultiplexer

To recover the symbols received, it is necessary to take into account that at the first receiving instant T_1 there is a version of the first symbol transmitted, where each copy is affected by the corresponding channel component. It occurs similarly for the last transmission instant of a layer, where various copies of the last symbol transmitted will be present at the receiver such that each copy is modified by one channel component.

Likewise, from the second to the penultimate receiving instant, each new symbol that comes in will be modified by some copy of the symbols that entered in previous time instants; in addition, in the case of intermediate symbols, this interference will be more accentuated. According to this, at the third time instant it may be seen that the third symbol that enters is modified by the two previous symbols that already entered in the matrix for their demodulation process.

Then, the D-BLAST technique for the 2×2 MIMO system carries out an average of the diagonals 1 and 2 of the symbol matrix Y_B , which implies that the mean value between the signal received by antenna R_{X1} at receiving instant T_1 and the signal received by antenna R_{X2} at receiving instant T_2 enables decoding

symbol s_1 according to equation 11. The symbol s_2 is decoded determining the mean value between the signal received by antenna R_{X1} at receiving instant T_2 and the signal received by antenna R_{X2} at receiving instant T_3 according to equation 12.

$$s_i = \frac{(s_1 h_{11} + n) + (s_2 h_{21} + s_1 h_{22} + n)}{2} \quad (11)$$

$$s_{i+1} = \frac{(s_2 h_{11} + s_1 h_{12} + n) + (s_2 h_{22} + n)}{2} \quad (12)$$

This procedure was applied in the 3×2 MIMO scheme. The average to obtain the first three symbols that were sent and the sequence they keep, which are shown below, are of vital importance.

$$s_i = \frac{(s_1 h_{11} + n) + (s_2 h_{21} + s_1 h_{22} + n)}{2} \quad (13)$$

$$s_{i+1} = \frac{(s_2 h_{11} + s_1 h_{12} + n) + (s_3 h_{21} + s_2 h_{22} + s_1 h_{23} + n)}{2} \quad (14)$$

$$s_{i+2} = \frac{(s_3 h_{12} + s_2 h_{13} + n) + (s_3 h_{23} + n)}{2} \quad (15)$$

These symbols are considered as estimates since they are distorted by the effect of the channel. Therefore, the channel coefficients determined in the channel estimation are used to eliminate this effect, multiplying times the conjugate transpose of the matrix with the coefficients obtained from the channel estimator.

In all cases where the number of transmitting antennas is larger than the number of receiving antennas, it will be necessary to complete the channel matrix with as many columns as the difference between ($N_{Tx} - N - Rx$) and dimension $N_{Tx} \times N_{Rx}$.

3. Analysis of Results

Due to the use of synchronization equipment, the distance between transmitter and receiver was around 3 meters, and to evaluate the behavior of the system, the power of the transmitter was modified with values from -30 dB to 15 dB preventing channel saturation. An additional radio equipment was used to generate a carrier with higher power to emulate the jamming effects in the transmission, to verify the operation for channel conditions such as great fading and multipath. The transmission frequency is 2.4 GHz, which coexists with the wifi network of the lab in which the experiments were carried out, thus producing continuous variations in the channel.

For the simulations carried out prior to the implementation, an indoor environment is considered where the distance effects are ignored to contrast it with the results obtained in the implementation. The evaluation of the simulation performance and experimentation

between spatial diversity and spatial multiplexing is described below. In addition, Table 6 summarizes the features of the equipment used in this implementation. It should be mentioned that the channel model used in the simulations corresponds to a channel with Rayleigh distribution, to consider the channel fading due to multipath; noise is also considered. The development of these simulations enabled establishing the processing of the radio signals to recover the message at the receiver.

Table 6. Parameters used in the implementation

Parameter	Value
Sampling rate IQ:	2,1 MSamples/s
Carrier Frequency:	2,4 GHz
Modulation:	4 QAM
Channel coder:	Convolutional, R=1/2
Transmitter gain:	15 dB
Receiver sensitivity:	10 dB
Types of Antennas Used:	Vertical Antennas for ISM band
Gain of Antennas:	6 dBi

Figures 5 and 6 show the disparity effect when $N_{Rx} < N_{Tx}$. When the system is symmetric MIMO (equal number of antennas), both the BER and SER are more optimal than when it is asymmetric. It was verified in a simulation environment, that a 2×2 MIMO based on Alamouti enables to reduce the impact of the BER.

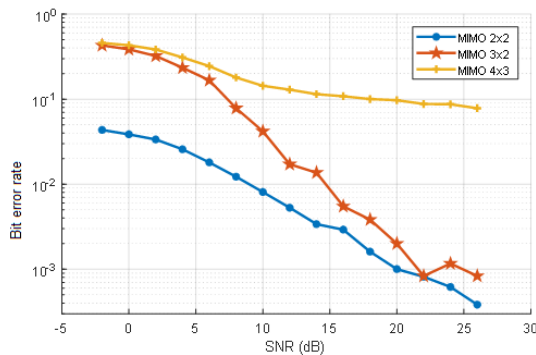


Figure 5. BER performance analysis in MIMO simulations

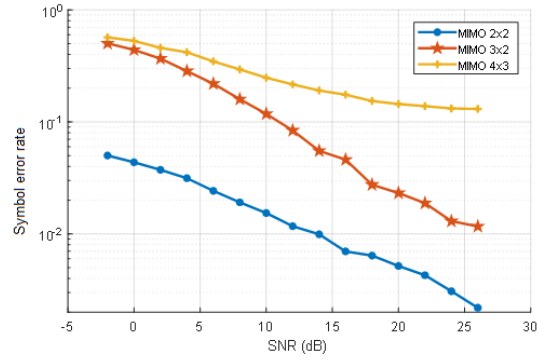


Figure 6. SER performance analysis in MIMO simulations

For the experimental approach, the same performance measures have been validated but with different techniques. Thus, in Figures 7 and 8 it may be compared the technique based on spatial diversity with Alamouti MIMO-10 vs. Spatial Multiplexing with D-BLAST MIMO.

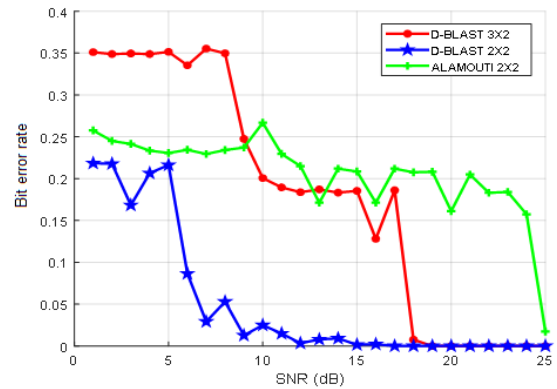


Figure 7. Experimental BER analysis between MIMO Alamouti and D-BLAST MIMO

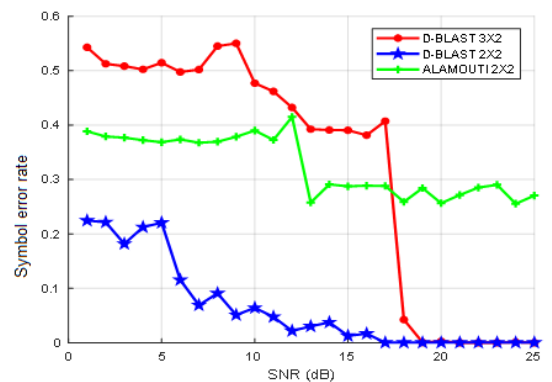


Figure 8. Experimental SER analysis between MIMO Alamouti and D-BLAST MIMO

Similarly, it may be observed that MIMO asymmetry deteriorates the system; nevertheless, the technique with BLAST Diagonal Matrices is better than traditional Alamouti space-time coding for MIMO in

around 10 dB. However, the symmetric and asymmetric D-BLAST MIMO systems are more robust than MIMO Alamouti; this is due to the mathematical treatment and the redundancy applied to the system to reduce the interference effects.

Another important point is that if the plots of all MIMO systems are compared, it may be observed that there is a higher symbol error rate than bit error rate for the same SNR value, which confirms the effectiveness of the convolutional coder despite the increased number of antennas. Nevertheless, it is clear that for larger MIMO systems, there is a higher probability of failure due to the complexity of the system even though the amount of data transmitted may be increased.

4. Conclusions

At present, the use of SDR systems is very important, since they are capable of processing large data chains generating a parallel processing, whose internal architecture is in the FPGAs designed to overcome this problem. The implementation of the 2×2 D-BLAST system (symmetric) was more efficient than the 3×2 D-BLAST system (asymmetric), showing a less significant bit error rate in the different MIMO schemes analyzed. In addition, a symmetric D-BLAST provides better spatial diversity since both the number of transmitting and receiving antennas may be increased, unlike Alamouti scheme in which only the number of receiving antennas may grow.

To implement D-BLAST or any other type of space-time coding for MIMO systems, it is recommended to take into account each of the coding and decoding processes described in this document. One of these fundamental processes is channel estimation, since its coefficients are required for a good wireless communication, for any number of antennas required both in the transmitter and in the receiver.

In this sense, channel coefficients should be arranged and maintained in sequence as shown in this work. If these coefficients are not the correct ones, channel estimation will be wrong, which will produce a significant bit error rate in low noise level. For future works it is recommended to try another system for channel estimation.

Finally, it should be indicated that for data transmission using D-BLAST MIMO with N_T transmitting antennas, it will be necessary to transmit the symbols in $2 \times (N_T - 1)$ symbol times, which should be analyzed for a large number of antennas if the D-BLAST operation does not come into conflict with the coherence time of the wireless channel. This is due to the fact that bandwidth is lost when redundancy is introduced in the symbol transfer.

References

- [1] S. Xu, S. Xu, and Y. Tanaka, "Dynamic resource reallocation for 5G with OFDMA in multiple user MIMO RoF-WDM-PON," 2016, pp. 480–484. [Online]. Available: <https://doi.org/10.1109/APCC.2015.7412561>
- [2] M. Danneberg, N. Michailow, I. Gaspar, M. Matthe, D. Zhang, L. L. Mendesy, and G. Fettweis, "Implementation of a 2 by 2 MIMO-GFDM transceiver for robust 5G networks," 2015, pp. 236–240. [Online]. Available: <https://doi.org/10.1109/ISWCS.2015.7454336>
- [3] N. Prasad and M. K. Varanasi, "Analysis and optimization of diagonally layered lattice schemes for MIMO fading channels," *IEEE transactions on information theory*, vol. 54, no. 3, pp. 1162–1185, 2008. [Online]. Available: <https://doi.org/10.1109/TIT.2007.915701>
- [4] B. Clerckx and Claude Oestges, *MIMO Wireless Networks*. Academic Press Publications, 2013. [Online]. Available: <https://doi.org/10.1016/C2010-0-66925-2>
- [5] Y. K. Chang, F. B. Ueng, and K. Z. Wu, "A novel MIMO-GFDM receiver for next generation communication," *Transactions on Emerging Telecommunications Technologies*, vol. 29, no. 6, pp. 1–15, 2018. [Online]. Available: <https://doi.org/10.1002/ett.3288>
- [6] M. Gupta and G. Murmu, "Experimental Study of Fading using Alamouti Space-Time Block Code," no. 1. IEEE, 2018, pp. 0–5. [Online]. Available: <https://doi.org/10.1109/SCEECs.2018.8546851>
- [7] A. Paulraj, R. Nabar, and D. Gore, *Introduction to Space-Time Wireless Communications*. Cambridge University Press, 2011, vol. 158. [Online]. Available: https://doi.org/10.1007/978-1-4419-6111-2_2
- [8] O. Shental, S. Venkatesan, A. Ashikhmin, and R. A. Valenzuela, "Massive BLAST: An architecture for realizing ultra-high data rates for large-scale MIMO," *IEEE WIRELESS COMMUNICATIONS LETTERS*, vol. 7, no. 3, pp. 404–407, 2017. [Online]. Available: <https://doi.org/10.1109/LWC.2017.2780079>
- [9] J. J. Mroczek, M. J. Gans, and L. L. Joiner, "Performance of frequency hopping d-blast mimo architecture using ldpc and bpsk," in *MILCOM 2015-2015 IEEE Military Communications Conference*. IEEE, 2015, pp. 860–865. [Online]. Available: <https://doi.org/10.1109/MILCOM.2015.7357553>

- [10] A. Sibille, C. Oestges, and A. Zanella, *MIMO: From Theory to Implementation*. Academic Press Publications, 2010. [Online]. Available: <https://bit.ly/3s2o9uk>
- [11] G. C. Daily and P. A. Matson, "Ecosystem services: From theory to implementation," *Proceedings of the National Academy of Sciences*, vol. 105, no. 28, pp. 9455–9456, 2008. [Online]. Available: <https://doi.org/10.1073/pnas.0804960105>
- [12] Y. Liu, B. Chen, J. J. Mroczek, J. E. Malowicki, and R. J. Michalak, "Robust mimo communications against antenna blockage and interference," in *MILCOM 2019-2019 IEEE Military Communications Conference (MILCOM)*. IEEE, 2019, pp. 7–12. [Online]. Available: <https://doi.org/10.1109/MILCOM47813.2019.9020916>
- [13] V. Garg, "Fourth generation systems and new wireless technologies," *en. Wireless Communications & Networking. Elsevier*, pp. 1–22, 2007.
- [14] N. T. Hieu, N. T. Tu, L. T. Danh, A. N. Duc, and B. H. Phu, "Design and implementation of MIMO-STBC systems on FPGA hardware," *International Conference on Advanced Technologies for Communications*, pp. 274–277, 2012. [Online]. Available: <https://doi.org/10.1109/ATC.2012.6404275>
- [15] J. Kaderka and T. Urbanec, "Time and sample rate synchronization of RTL-SDR using a GPS receiver," in *2020 30th International Conference Radioelektronika (RADIOELEKTRONIKA)*, 2020, pp. 4–7. [Online]. Available: <https://doi.org/10.1109/RADIOELEKTRONIKA49387.2020.9092398>
- [16] G. Soni, G. Kaur, and V. K. Banga, "Implementation & BER analysis of 2x2 MIMO Using USRP 2920- universal software radio peripheral," in *2016 Second International Conference on Computational Intelligence Communication Technology (CICT)*. IEEE, 2016, pp. 523–527. [Online]. Available: <https://doi.org/10.1109/CICT.2016.109>
- [17] V. S. Muradi, R. K. Paithane, A. Ahmed, and A. Pawar, "Spectrum sensing in cognitive radio using Labview and NI USRP," in *2018 2nd International Conference on Inventive Systems and Control (ICISC)*. IEEE, 2018, pp. 1316–1319. [Online]. Available: <https://doi.org/10.1109/ICISC.2018.8399019>
- [18] A. Yanza-Verdugo, C. Pucha-Cabrera, and J. Inga-Ortega, "Compressive Sensing Based Channel Estimator and LDPC Theory for OFDM using SDR," *Ingenius. Revista de Ciencia y Tecnología*, vol. 23, no. 1, pp. 74–85, 2020. [Online]. Available: <https://doi.org/10.17163/ings.n23.2020.07>
- [19] N. Narukawa, T. Fukushima, K. Honda, and K. Ogawa, "64 x 64 MIMO antenna arranged in a daisy chain array structure at 50 Gbps capacity," in *2019 URSI International Symposium on Electromagnetic Theory (EMTS)*. URSI, 2019, pp. 2019–2022. [Online]. Available: <https://doi.org/10.23919/URSI-EMTS.2019.8931517>
- [20] R. Prieto, A. Abril, and A. Ortega, "Experimental Alamouti-STBC Using LDPC Codes for MIMO Channels over SDR Systems," in *2017 IEEE 30th Canadian Conference on Electrical and Computer Engineering (CCECE)*. IEEE, 2017, pp. 1–5. [Online]. Available: <https://doi.org/10.1109/CCECE.2017.7946842>
- [21] V. Soria, G. V. Arevalo, P. Avila, F. Tello, and C. G. Santamaria, "Performance comparison of 2x2 and 4x4 V-BLAST and Alamouti MIMO systems," in *2018 IEEE 3rd Ecuador Technical Chapters Meeting, ETCM 2018*, 2018, pp. 18–21. [Online]. Available: <https://doi.org/10.1109/ETCM.2018.8580317>
- [22] J. J. Anguís Horno, *Redes de Área Local Inalámbricas: Diseño de la WLAN de Wheelers Lane Technology College*. Escuela Superior de Ingenieros Universidad de Sevilla, 2008. [Online]. Available: <https://bit.ly/3IFbsM9>
- [23] M. Sellathurai and S. Haykin, *Space-Time Layered Information Processing for Wireless Communications*. Wiley & Sons, 2009. [Online]. Available: <https://bit.ly/3oPIjG3>
- [24] J. R. Hampton, *Introduction to MIMO communications*. Cambridge university press, 2013. [Online]. Available: <https://bit.ly/3DQyh2>
- [25] V. Puig Borrás, "Simulación computacional y paralelización de un sistema de comunicaciones inalámbrico MIMO: Estimación de canal y decodificación de señales," Master's thesis, Universidad Politécnica de Valencia, 2011. [Online]. Available: <https://bit.ly/3IWIWlc>
- [26] Y. S. Cho, J. Kim, W. Y. Yang, and C. G. Kang, *MIMO-OFDM Wireless Communications with MATLAB*. Wiley & Sons, 2010, vol. 11, no. 3. [Online]. Available: <https://bit.ly/3m3QgFN>